Investigation of Stability Property of Graph Neural Network Architectures under Domain Perturbations

Authors Khoa M. Nguyen
nmkhoa057@gmail.com

Affiliations DELFT UNIVERSITY OF TECHNOLOGY

Objective

The objective of this study is to answer the question of **"how domain perturbations affect different types of GNN architectures?"** by conducting an investigation into the architectures that are required to be stable against stochastic perturbation, and in the project's scope, Traffic forecasting problems. The stability property of each architecture will be quantified and put on comparison to determine how they perform under topology shifts.

Methodology

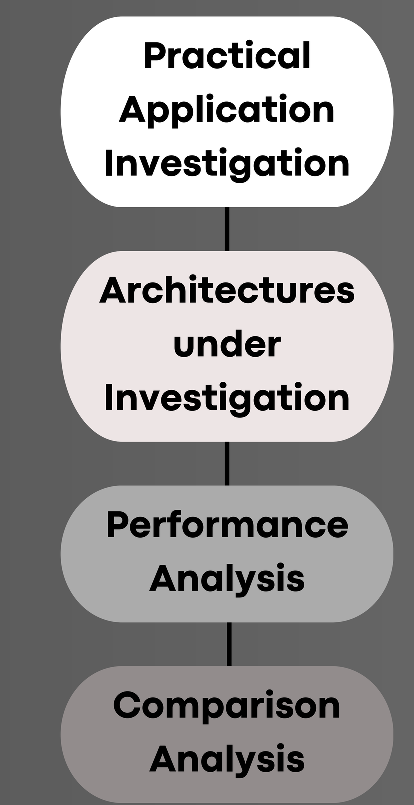

Figure 1: The research methodology employed

Practical Aplication Investigation

Graphs, graphs are everywhere, appearing in applications ranging from the well-known fraud detection in X [2] to graph recommendation systems [3]. While many of these problems have been thoroughly researched over the past decade, the application of Graph Neural Networks (GNN) to traffic forecasting is still a relatively recent development.

Background

Traffic forecasting problems using standard PEMS-BAY dataset constructs by a graph G = (V, E) where V and E stand for vertices (sensors) and edges (road link), respectively, and represented by an adjacency matrix with pairwise distance between 325 sensors (see figure 11). Each of the sensor records the speed and number of vehicles through every 5-minute interval, divided into 12 time steps, and our task is to predict the next time step.

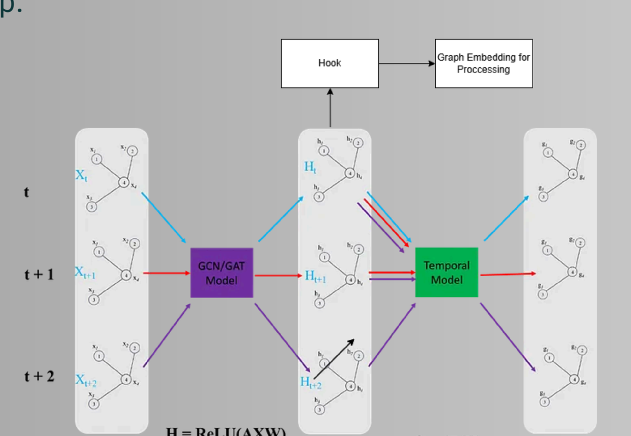

Figure 1: The GNN method to learn this problem can be divided into spatial and temporal parts. While the temporal capturing mechanism is well-studied [3], more investigation is needed to further study the spatial capturing mechanism. Hence, we place a hook to capture the resulting graph after feedforward the input through the spatial capturing layer.

Architectures under Investigations

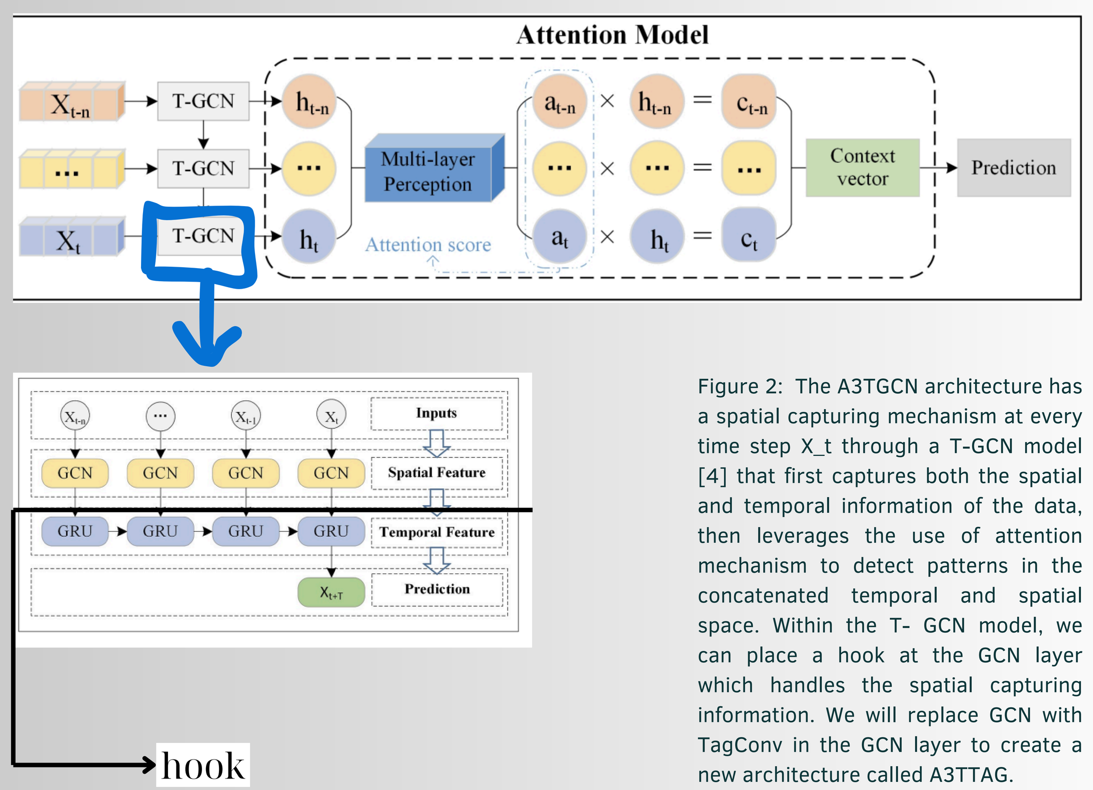

Figure 2: The A3TGCN architecture has a spatial capturing mechanism at every time step X_t through a T-GCN model [4] that first captures both the spatial and temporal information of the data, then leverages the use of attention mechanism to detect patterns in the concatenated temporal and spatial space. Within the T- GCN model, we can place a hook at the GCN layer which handles the spatial capturing information. We will replace GCN with TagConv in the GCN layer to create a new architecture called A3TTAG.

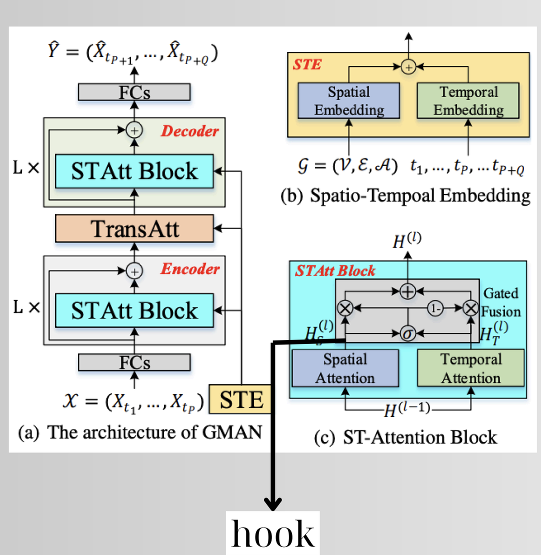

Figure 3: Graph Multi-Attention Network (GMAN) [5] leverages the use of the attention mechanism in GATConv in both spatial and temporal capturing domains. It follows an encoder-decoder structure, which consists of L (L ∈ N) Spatial-Temporal Attention Block (STAtt). We will focus on the spatial capturing mechanism of the model, which happens in a STAtt block. A hook will be implemented to extract the spatial attention described here, in both encoder and decoder.

Performance Analysis Results (of 10% perturbation)

Metric scores for stability property of spatial graph embedding

Cosine Similarity

$$\text{Cosine Similarity} = \cos(\theta) = \frac{\mathbf{A}\cdot\mathbf{B}}{\|\mathbf{A}\|\|\mathbf{B}\|}$$

Euclidean Distance

$$d(\mathbf{A},\mathbf{B}) = \sqrt{\sum_{i=1}^{n}(A_i - B_i)^2}$$

We represent **A** as graph embedding before the in- put graph being perturbed, while **B** is the graph embedding of the perturbed input graph

Dataset

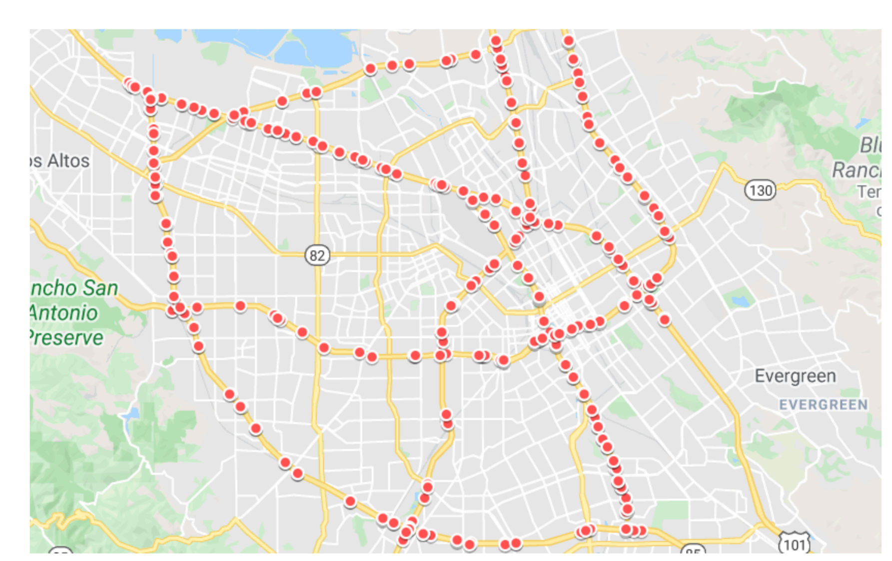

Figure 11: PEMS-BAY visualization [6] of 325 sensors distributed across California

A3TGCN

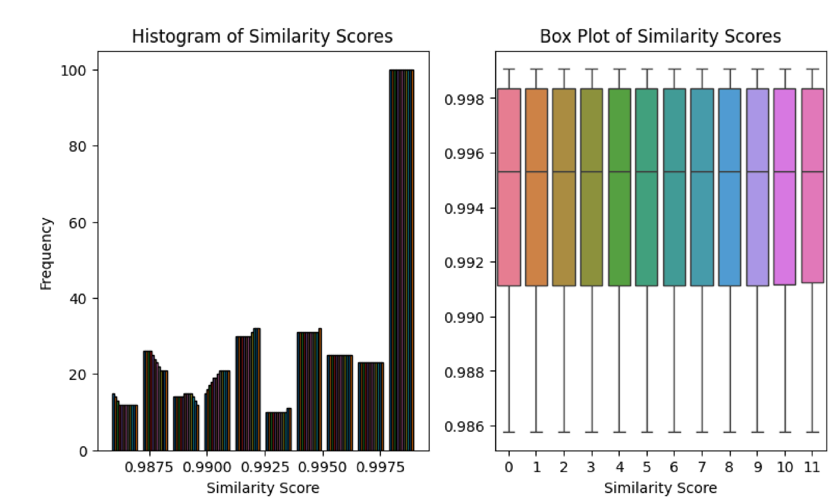

Figure 4: the graph embedding similarity scores of cosine similarity are consistent, with the fluctuations shown to be minor, ranging from 0.98 to 1 (highly stable)

Figure 5: The similarity score of euclidean distance following with cosine similarity fluctuates only around 0.75 and 1.5, display- ing a high stability property in both metric scores.

A3TTAG

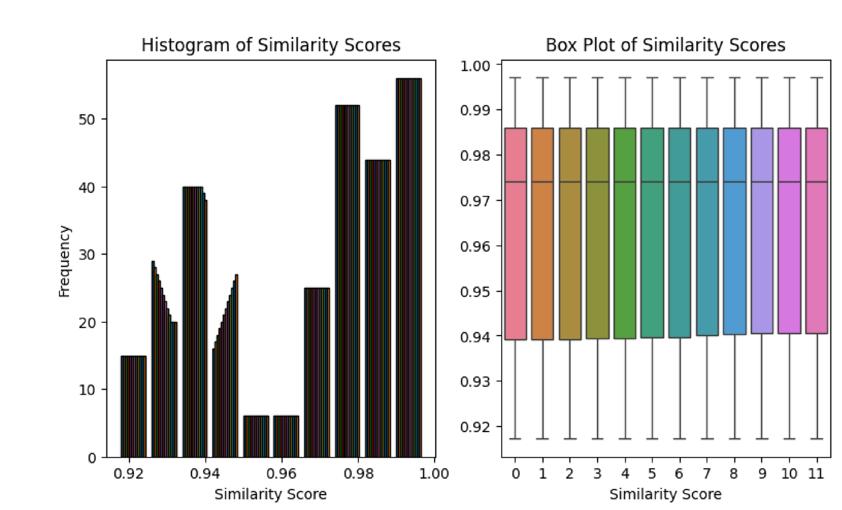

Figure 6: The graph embedding similarity scores of cosine similarity are pertained, with the fluctuations are shown to be minor, ranging from 0.994 to 1 (highly stable).

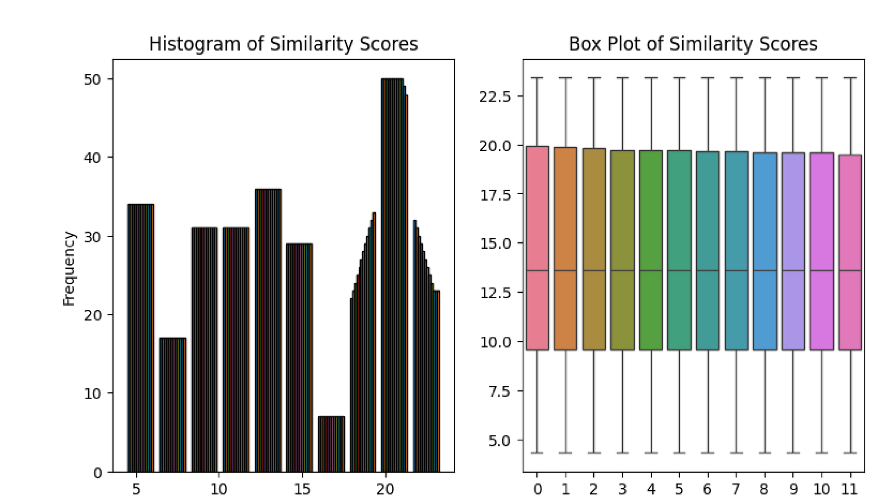

Figure 7: The similarity score of euclidean distance differs significantly for A3TTAG, which fluctuates around the region of 5 and 23, followed with cosine similarity fluctuates only around 0.75 and 1.5

GMAN

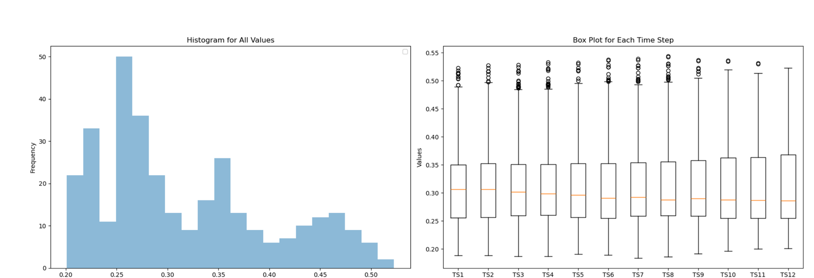

Figure 8: 10% perturbation, it ranges from 0.25 to 0.35. This significant difference in cosine similarity scores highlights substantial disparities in the spatial embeddings between perturbed and non-perturbed graphs within the GMAN architecture

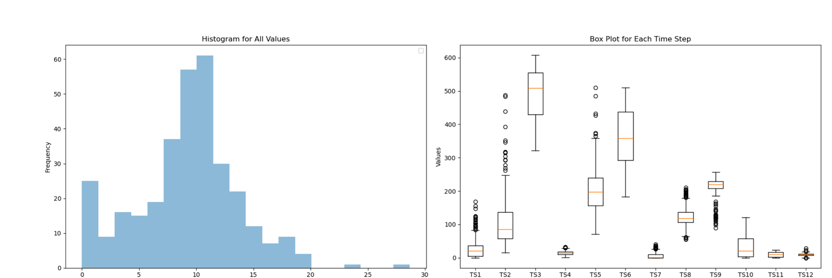

Figure 9: with 10% perturbation, the scores range from 300 to 600, showing a dramatic difference compared to the 10% perturbation of both A3TGCN/A3TTAG architectures. These frequency ranges highlight the unstable nature of the spatial attention mechanism within the GMAN architecture

Comparison Analysis

Evaluation metric for final output

$$\text{RMSE} = \sqrt{\frac{1}{n}\sum_{i=1}^{n}(y_i - \hat{y}_i)^2}$$

Where y_i is the ground truth, y^_i is the model prediction of the perturbed input

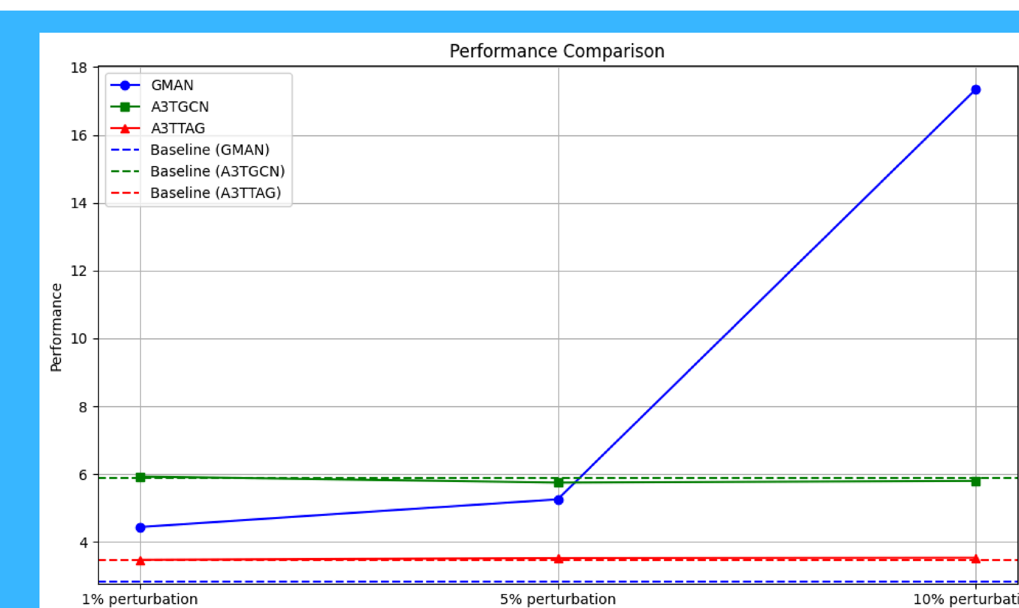

Figure 10: To improve the illustration of the connection between the per- turbation ratio and each model's final output performance, we add a 5% perturbation to the equation. The results show that A3TGCN and A3TTAG perform better than GMAN under stochastic edge perturbation. On the other hand, GMAN per- forms better at baseline than these two architecture

Conclusion

In conclusion, we presented a comparative analysis of each model's overall performance and made preliminary findings regarding the connection between spatial graph embeddings and overall graph performance following the stochastic perturbation. Although there is a lack of prior research on the relationship between spatial embedding and overall graph performance, our analysis has revealed significant differences in model performance, and display that some models are superior under stochastic perturbation.

Limitations

The number of architectures under investigation is limited due to in appropriate equipment for a large learning task such as Traffic Forecasting. To fully comprehend the relationship between spatial embedding and overall graph performance, more models and settings should be investigated to draw a broader conclusion on these relationships

References

[1] Zhan Gao, Elvin Isufi, and Alejandro Ribeiro. Stability of graph convolutional neural networks to stochastic perturbations, 2021.
[2] Loukas Ilias and Ioanna Roussaki. Detecting malicious activity in twitter using deep learning techniques. Ap- plied Soft Computing, 107:107360, 2021.
[3] Rex Ying, Ruining He, Kaifeng Chen, Pong Eksombat- chai, William Hamilton, and Jure Leskovec. Graph con- volutional neural networks for web-scale recommender systems, 06 2018
[4] Chuanpan Zheng, Xiaoliang Fan, Cheng Wang, and Jianzhong Qi. Gman: A graph multi-attention network for traffic prediction, 2019
[5] Rex Ying, Ruining He, Kaifeng Chen, Pong Eksombatchai, William Hamilton, and Jure Leskovec. Graph convolutional neural networks for web-scale recommender systems, 06 2018
[6] Yaguang Li, Rose Yu, Cyrus Shahabi, and Yan Liu. Dif- fusion convolutional recurrent neural network: Data- driven traffic forecasting, 2018.